UNRAVELING THE VISCOSITY-MEDIATED COUPLING EFFECT IN BIOMIMETIC HAIR SENSOR ARRAYS

R.K. Jaganatharaja, H. Droogendijk, S. Vats, B. Hagedoorn, C.M. Bruinink and G. Krijnen
University of Twente, Enschede, The Netherlands

ABSTRACT

A dedicated microfabricated chip consisting of artificial hair sensors was realized and used to controllably and reliably investigate viscous coupling between the hair sensors. The experimental results confirm the presence of coupling effects between hair sensors when placed too close to each other. The results present significant insights in optimal array arrangements for high spatial resolution by preservation of the hair-sensors uncoupled (individual) responses.

INTRODUCTION

Biological organs and processes found on different species of animals have been a source of inspiration for engineers. Mechano-sensing as seen in nature is among these interesting phenomena and has attracted significant scientific interest [1-7]. Mechano-receptive hair-sensors, found on crickets and other insects (Figure 1), are among the most energy-efficient sensory systems in nature [1]. Recently, these sensitive hair sensors have inspired MEMS engineers [2,3] to develop novel flow-sensor arrays.
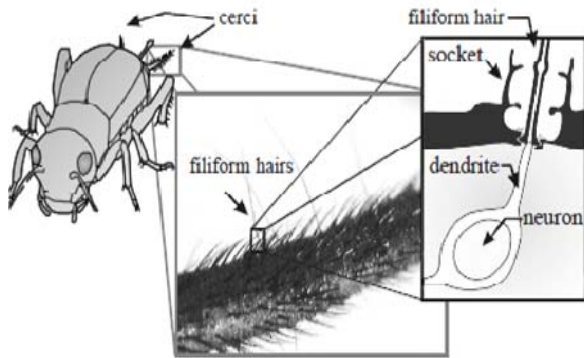

Figure 1: Mechano-receptive hair-sensor as found on the cerci of a cricket. Enlarged SEM image shows the high-density of filiform hairs. [SEM Courtesy: J. Casas, IRBI, Univ. of Tours, France]

Crickets have evolved with a highly sensitive system of mechano-receptive hairs that are able to pick up low-frequency air flows [1]. The sensory hairs are radially distributed on a pair of special appendages called cerci, located at the back of the abdomen of the cricket. These hairs are used to sense approaching predators and, therefore, play a predominant role in the escape mechanism of crickets. We successfully engineered hair-based flow sensor arrays inspired by these cricket mechano-sensors. Making use of state-of-the-art MEMS technology, high density

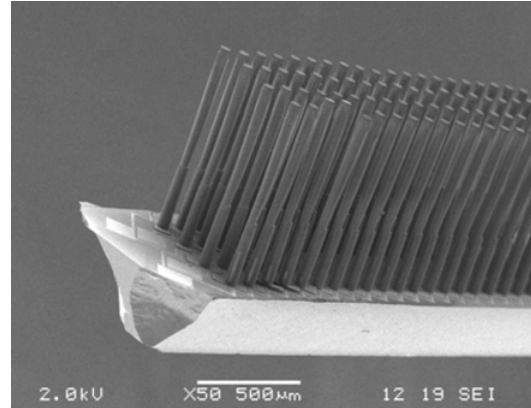arrays of SU-8 based artificial hair sensors have been successfully fabricated recently (Figure 2) [3].

Figure 2: SEM image of a dense-array of artificial hair sensors, designed to sense low-frequency air flows [3].

Viscosity-mediated coupling effect

Despite the successful sensor-array development, several characteristics of the cercal hairs in an array - like viscous coupling, still remain unknown or less understood by scientists. One unexplained and interesting aspect is related to the occurrence of sensory filiform hairs in high-densities and the associated effects on single hair-sensor performance [4]. The impact of one hair sensor on its neighbors is mediated by viscous coupling [1-a,5]. This effect has been debated in literature, both from theoretical and experimental viewpoints [4-6], but poses many practical difficulties for experimental studies on living animals [4].

Arrays of high-density artificial hair-sensors are required for high spatial resolution in flow signature detection applications. The presence of viscous coupling impacts the sensitivity of the hair sensors. Hence, investigation of viscous coupling between artificial hair-sensors can make a significant contribution to the design of optimal arranged sensor arrays. Simultaneously it helps biologists to further their understanding of the functioning and bauplan of such high density sensory arrays as found on crickets, appreciating the difficulties to investigate viscous coupling effects on the actual cerci. With the major advantage of exerting control over the operation and geometry of the artificial sensory hairs, a wide range of experimental characterizations is now possible. The aim of this work is to study the presence of viscous coupling between artificial hair sensors. Initially, the parameters which play a major role in viscous coupling are identified. Using this knowledge, an experimentation platform comprising several artificial hairs

arranged in specific patterns is designed and realized. The first set of results is presented here.

VISCOUS COUPLING MODEL

Viscosity-mediated coupling effects between mechano-receptive hairs has been studied and modeled in literature [4-6]. Since a comparable size-match exists between the actual cricket hairs and artificial hair sensors, models on viscosity-mediated coupling can be applied to our systems, using the actual parameters. A computational model [6] and experimental results using particle image velocimetry [4], exclusive to our artificial hair sensors are discussed in detail.

Each hair sensor on the chip consists of a long hair centrally placed on a thin, suspended membrane. In the presence of oscillating air-flows drag-forces are exerted on the hair causing a moment and, consequently, a tilt of the membrane. The hair-sensor can be modeled as an inverted-pendulum, a second-order mechanical system. Derived from the angular momentum equation of the hair sensor, the amplitude of the hair sensor response (i.e. rotational angle of the membrane) is given as [7]:

$$\theta(\omega) = \frac{T_d}{J} \cdot \frac{1}{\left(\omega_0^2 - \omega^2 + i\omega(R/J)\right)} \qquad (1)$$

where T_d is the drag-torque acting on the hair, ω is the radial frequency, J is the hair moment of inertia, S is the torsional spring constant of the suspensions, R is the torsional resistance of the hair sensor and ω_0 is the resonance frequency of the system given by $(S/J)^{0.5}$. In general R and J will contain effects related to the boundary layer around the hairs (added mass, see [1]).

Presence of a perturbing hair in the proximity of a reference sensor will affect the flow-induced drag-torque exerted on both. While the impact of this flow disturbance depends on many factors [5,6] only the predominant parameters such as the geometry of the hairs (length L, diameter D) and normalized distance between the hairs (s/D) are considered in this experimental characterization.

By measuring the reference hair sensor response, in presence and absence of a perturbing hair, the effect of viscosity-mediated coupling can be experimentally investigated. To quantify the coupling effect, the coupling coefficient κ is defined as [4-6]:

$$\kappa = \frac{\theta_r - \theta_p}{\theta_r} \qquad (2)$$

where θ_p and θ_r are the reference hair sensor responses in the presence and absence of a perturbing hair, respectively.

DESIGN AND FABRICATION

A novel chip is designed consisting of hair sensors arranged in various patterns by systematically varying: (i) the inter-hair distance (s), (ii) the length of the hairs (L) and (iii) the number of perturbing hairs, present in front of the reference hair sensor and (iv) by either having the perturbing hair fixed on the substrate or on a movable membrane. The inter-hair distance s is usually scaled in terms of the hair diameter D and on the chip, the hairs were placed at center-to-center distances ranging from $2D$ - $8D$. Long hairs were designed to be ~700 μm while short hairs were ~350 μm. All sensors feature identical torsion beams (length: 100 μm, width: 6 μm and thickness: 1 μm) and membrane designs (each sensor membrane has two plates and each plate has dimensions: 100 μm x 50 μm.)
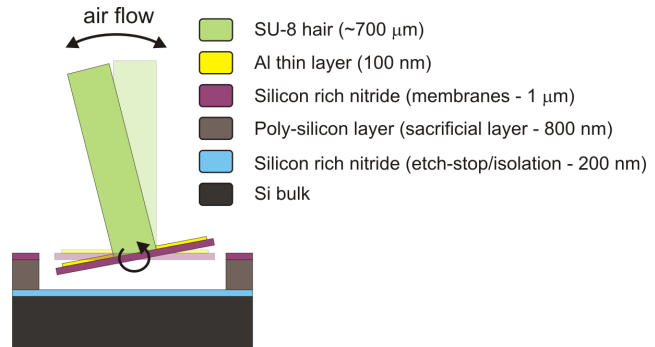

Figure 3: Schematic of the artificial hair sensor [3]: an SU-8 hair acts as a flow-receptor, mounted on the suspended silicon rich nitride membrane. An aluminum thin layer serves for optical measurement of the membrane tilt.

The chip is fabricated using advanced MEMS technologies [3] and a schematic of the hair sensors is shown in figure 3. First, a protective layer of silicon-rich nitride is deposited using LPCVD, followed by the deposition of a ~800 nm thick poly-silicon layer. This poly-silicon layer acts as a sacrificial layer for the final release of the structures. A ~1 μm thick silicon-rich nitride layer is deposited and patterned to form the sensor membranes and springs. The membrane is covered by a thin layer of Aluminum (which functionally serves as the top electrode of the sensor capacitors, but in the current studies, only serves as a reflecting surface during optical characterization). Long hairs are made by two subsequent layers of SU-8 (of ~350 μm each) using standard lithography techniques. Finally the sensor membrane is released by selective-etching of the sacrificial poly-silicon layer (Figure 3) using a XeF$_2$ etcher. Figure 4 shows SEM images of a successfully realized chip.
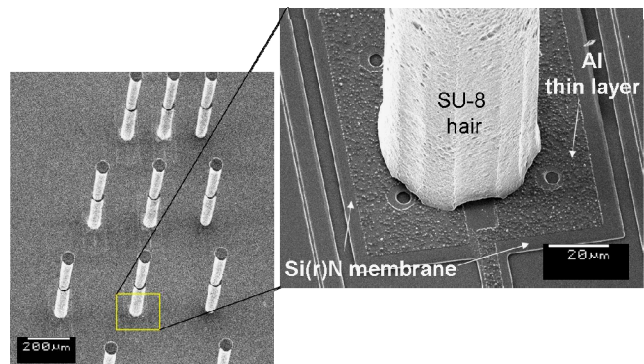

Figure 4: SEM image showing a portion of the novel chip for characterization of viscosity-mediated coupling. The hair sensors are arranged at various inter-hair distances.

CHARACTERIZATION

Measurement setup

The hair-sensors are exposed to the near-field of a small loudspeaker (diameter, 4 cm) and their mechanical responses are optically characterized by a laser vibrometer (Polytec, MSA400). Figure 5 shows a schematic of the measurement setup. In order to calibrate the generated flow field, the loudspeaker is first placed under the laser vibrometer measuring the movement of its membrane under given actuating voltages and frequencies.
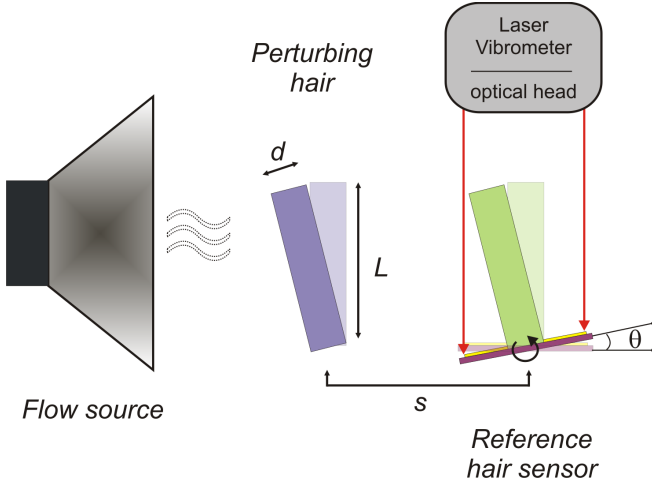

Figure 5: Experimental setup comprising of a flow source (loud speaker), the chip with artificial hair sensors and the laser vibrometer. The rotational angle of the sensor membrane is measured in presence and absence of a flow perturbing hair.

The sensor chip is then placed on a steady platform under the laser vibrometer. The loudspeaker is mounted on a separate stand to avoid any unwanted coupling of mechanical vibrations to the measurement system. The sensors were always placed in such a way that the hairs were exposed to the flow from the center of the loudspeaker membrane (where the flow is assumed to have high uniformity [5]) and at the nearest possible position from the loudspeaker to ensure all the measurements were performed in the near-field of the loudspeaker.

Using the laser vibrometer the dynamics of the hair-sensor under given flow fields were accurately measured. Scan points were placed (using software) on both edges of the suspended membranes (on top of the Aluminum layers, for better reflectivity) and maximum displacements were measured. From these displacements and the distance between the scan points, the rotational angles were calculated.

In order to characterize the viscosity-mediated coupling between the hair sensors measurements were performed on a reference hair sensor, with the presence of a second hair sensor and repeated in the absence of it (by manual removal). For both measurements the corresponding rotational angle of the reference sensor was calculated and hence, the coupling coefficient was determined. However, the manual removal of the perturbing hair is tedious and care was taken

to ensure that both measurements took place in near-identical conditions. The hair was removed using a micro-probe and the chip was placed back into the system, exactly at the same position as before. The precise placement was aided by the scan points of the laser vibrometer software.

Viscous coupling between the hair sensors

Figure 6 shows the normalized frequency response of a reference hair sensor, with and without a perturbing hair (θ_p and θ_r, respectively). The perturbing hair, which is free-moving like the reference hair sensor, was at a distance of ~150 μm from the reference hair. Both hairs were of same length (~700 μm). The measurements were in good agreement with the model.
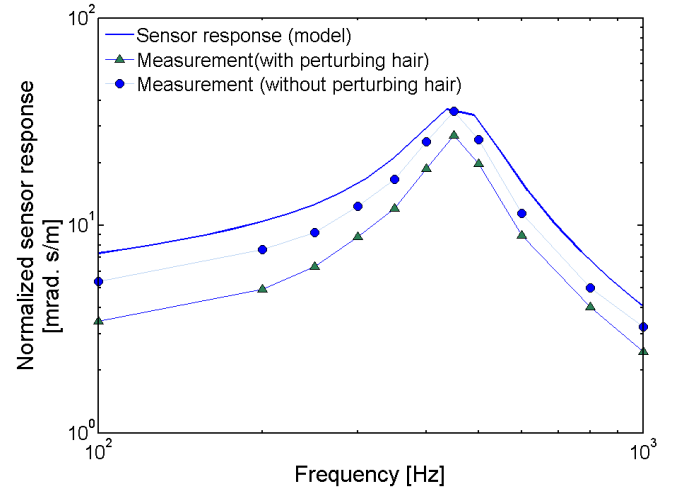

Figure 6: Normalized responses of the reference hair sensor in presence and absence of a free-moving perturbing hair respectively, placed at 150 μm (s/D ~2.14).

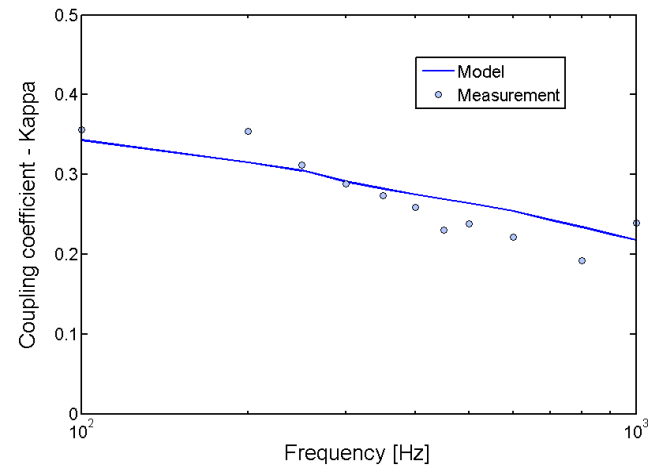*Figure 7: Coupling coefficient between the reference hair-sensor and the perturbing hair (free-moving) placed at 150 μm (s/D~2.14). Strong coupling (κ > 0.3) is observed at low frequencies (<500 Hz). The measurement result is in good agreement with the model.*

Based on the sensor responses shown in figure 6, the coupling coefficient is calculated using equation (2). The

result is shown in figure 7 and is in good agreement with the model. The coupling effect is predominant ($\kappa > 0.3$) at lower frequencies (< 500 Hz). This clearly confirms the presence of viscosity-mediated coupling between hair sensors when arranged in dense patterns.
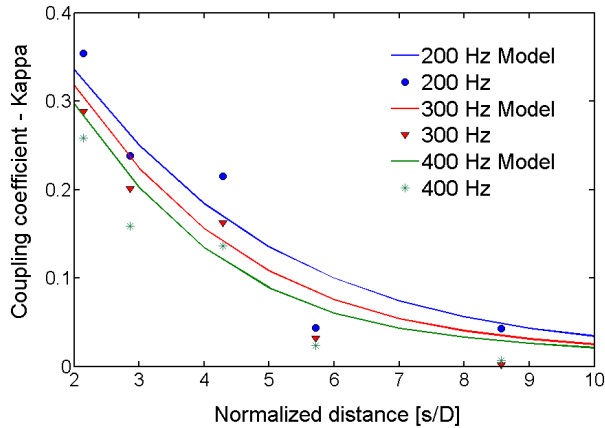

Figure 8: Measurement results showing significant coupling at smaller inter-hair distances (and at lower flow frequencies). The perturbing hair was free-moving and of same length as the reference hair. D is the diameter of both hairs (~70 μm).

Figure 8 shows the coupling coefficient determined for a reference hair sensor placed at various distances from a free-moving perturbing hair. The results indicate a significant coupling effect ($\kappa > 0.2$) due to the presence of the perturbing hair at closer normalized distances ($s/D < 4$). As observed before, this effect is especially prominent at low frequencies (<400 Hz).
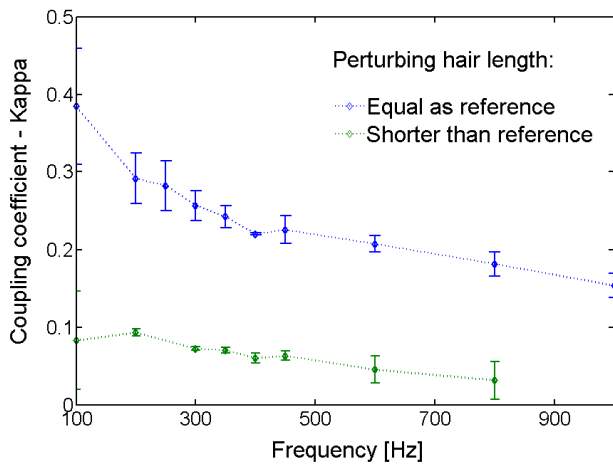

Figure 9: Results indicating that the length of the perturbing hair has significant effect on viscous coupling to the reference hair. Both perturbing hairs (equal and half the length of the reference hair, respectively) were fixed. The reference hair was at a distance of 150 μm (s/D ~ 2.14)

Figure 9 compares the effect of a fixed perturbing hair on the extent of viscous coupling on the reference hair for the case of short normalized distance ($s/D \sim 2.14$). Two different cases are considered here: (i) both hairs are of equal length, (ii) the perturbing hair is shorter than the reference hair. Significant effects are observed when the hairs are of equal length. A short perturbing hair has less impact on a longer reference hair ($\kappa < 0.1$).

CONCLUSIONS

A microfabricated chip featuring artificial hair sensors arranged in specifically designed patterns to characterize the presence of viscosity-mediated coupling is presented. The results show significant coupling effects between hairs, when placed close to each other and at lower flow frequencies. The length of the perturbing hair has a significant coupling effect on the reference hair sensor. The measurements were in good agreement with the theoretical models. These results provide important guidelines towards optimal sensor array designs while simultaneously confirming and clarifying existing biophysical effects in closely-packed hair-sensor arrays

REFERENCES

[1] (a) J.A. Humphrey and F.G. Barth, *Advances in Insect Physiology*, 34 (2008), pp. 1-80; (b) T. Shimozawa, *J. Murakami, T. Kumagai*, "Structural scaling and functional design of the cercal wind-receptor hair of cricket", *J. Comp. Physiol. A* (1998) Vol. 183, pp. 171–186

[2] (a) Y. Ozaki et al, *Proc. IEEE Int. Conf. MEMS* (Miyasaki, Japan) 2000, pp. 531-536; (b) J. Zou et al., *J. Microelectromech. Syst.*, 10(2001), pp. 302-309;

[3] C.M. Bruinink, R.K. Jagnatharaja, M.J. de Boer, E. Berenschot, M.L. Kolster, T.S.J. Lammerink, R.J. Wiegerink, G.J.M. Krijnen, "Advancements in techno-logy and design of biomimetic flow-sensor arrays", *Proc. IEEE Int. Conf. MEMS* (Sorrento, Italy) 2009, pp. 152-155.

[4] J. Casas, T. Steinmann, G. Krijnen, „Why do insects have such a high density of flow sensing hairs? Insights from the hydromechanics of biomimetic MEMS sensors", *J. R. Soc. Interface*, Vol. 7, pp. 1487-1495, 2010

[5] B. Bathellier, *F.G. Barth, J.T. Albert, J.A.C. Humphrey*, "Viscosity-mediated motion coupling between pairs of trichobothria on the leg of the spider Cupiennius salei", *J. Comp. Physiol A.*, vol. 191, pp. 733-746, 2005.

[6] G.C. Lewin, *J. Hallam*, „A computational fluid dynamics model of viscous coupling of hairs", *J. Comp. Physiol. A, 196(6) (2010)*, pp. 385-395.

[7] G. Krijnen, A. Floris, M. Dijkstra, T. Lammerink, R.J. Wiegerink, "Bio-mimetic micromechanical adaptive flow-sensor arrays", *Proc. of SPIE Europe Microtechnologies for the New Millennium, Gran Canary, Spain* (2007).